THE JOURNAL OF BIOLOGICAL CHEMISTRY VOL. 282, NO. 11, pp. 7939–7949, March 16, 2007

Paraquat Increases Cyanide-insensitive Respiration in Murine Lung Epithelial Cells by Activating an NAD(P)H:Paraquat Oxidoreductase

*IDENTIFICATION OF THE ENZYME AS THIOREDOXIN REDUCTASE**

Received for publication, December 26, 2006 Published, JBC Papers in Press, January 17, 2007, DOI 10.1074/jbc.M611817200

Joshua P. Gray[‡], Diane E. Heck[§], Vladimir Mishin[§], Peter J. S. Smith[¶], Jun-Yan Hong[‖], Mona Thiruchelvam[‡], Deborah A. Cory-Slechta[‡], Debra L. Laskin[§], and Jeffrey D. Laskin[‡1]

From the [‡]Department of Environmental and Occupational Medicine, University of Medicine and Dentistry of New Jersey-Robert Wood Johnson Medical School, Piscataway, New Jersey 08854, [§]Department of Pharmacology and Toxicology, Rutgers University, Piscataway, New Jersey 08854, [¶]Biocurrents Research Center, Marine Biological Laboratory, Woods Hole, Massachusetts 02543, and [‖]University of Medicine and Dentistry of New Jersey-School of Public Health, Piscataway, New Jersey 08854

Pulmonary fibrosis is one of the most severe consequences of exposure to paraquat, an herbicide that causes rapid alveolar inflammation and epithelial cell damage. Paraquat is known to induce toxicity in cells by stimulating oxygen utilization via redox cycling and the generation of reactive oxygen intermediates. However, the enzymatic activity mediating this reaction in lung cells is not completely understood. Using self-referencing microsensors, we measured the effects of paraquat on oxygen flux into murine lung epithelial cells. Paraquat (10–100 μM) was found to cause a 2–4-fold increase in cellular oxygen flux. The mitochondrial poisons cyanide, rotenone, and antimycin A prevented mitochondrial- but not paraquat-mediated oxygen flux into cells. In contrast, diphenyleneiodonium (10 μM), an NADPH oxidase inhibitor, blocked the effects of paraquat without altering mitochondrial respiration. NADPH oxidases, enzymes that are highly expressed in lung epithelial cells, utilize molecular oxygen to generate superoxide anion. We discovered that lung epithelial cells possess a distinct cytoplasmic diphenyleneiodonium-sensitive NAD(P)H:paraquat oxidoreductase. This enzyme utilizes oxygen, requires NADH or NADPH, and readily generates the reduced paraquat radical. Purification and sequence analysis identified this enzyme activity as thioredoxin reductase. Purified paraquat reductase from the cells contained thioredoxin reductase activity, and purified rat liver thioredoxin reductase or recombinant enzyme possessed paraquat reductase activity. Reactive oxygen intermediates and subsequent oxidative stress generated from this enzyme are likely to contribute to paraquat-induced lung toxicity.

Exposure of humans and animals to toxic doses of paraquat (1,1′-dimethyl-4,4′-bipyridylium) is known to damage the lung leading to pulmonary edema and hypertension, acute respiratory distress syndrome, and progressive lung fibrosis (1). In target cells paraquat undergoes redox cycling which may contribute to its toxic actions. Several mammalian NADPH oxidases have been identified as potential inducers of paraquat redox cycling including cytochrome P450 reductase and nitric-oxide synthase (2, 3). These enzymes generate a reduced paraquat radical that can act as an electron donor (4) (see Reaction 1). Reacting rapidly with molecular oxygen, the paraquat radical recycles back to paraquat and in the process forms highly toxic oxidants including superoxide anion, hydrogen peroxide, hydroxyl radicals, and in the presence of nitric oxide, peroxynitrite (5–7). Cellular damage generated by these oxidants, including lipid peroxidation, may be important in paraquat-induced lung damage (8, 9).

Redox cycling reactions are known to consume significant quantities of oxygen (10–12). In cells, this has the potential to reduce levels of oxygen available for metabolic processes resulting in oxidative stress and toxicity (13). Previous studies have demonstrated that paraquat can stimulate oxygen uptake by microsomes from rat and rabbit liver and rabbit lung as well as rabbit lung slices, alveolar macrophages, and lung fibroblasts and in *Escherichia coli* (14–21). In intact cells this was only observed in the presence of the respiratory chain inhibitor cyanide (18). Based on these findings, it has been suggested that paraquat functions by diverting electron flow from cyanide-sensitive respiration (18). In the present studies we report that paraquat treatment of murine lung epithelial cells markedly increases the flux of oxygen into cells in a process that is independent of cyanide-sensitive respiration. These results are consistent with enhanced oxygen utilization during paraquat redox cycling (22). We also report that redox cycling appears to be initiated by a one-electron reduction of the herbicide by a specific NAD(P)H oxidase. This enzymatic activity was purified and shown to generate paraquat radical and to mediate production of ROI.[2] Thioredoxin reductase, an important antioxidant

* This work was supported in part by National Institutes of Health Grants U54AR055073, ES006897, CA100994, CA093798, ES003647, ES010791, ES004738, GM034310, RR001395, and ES005022. The costs of publication of this article were defrayed in part by the payment of page charges. This article must therefore be hereby marked "*advertisement*" in accordance with 18 U.S.C. Section 1734 solely to indicate this fact.

[1] To whom correspondence should be addressed: Dept. of Environmental and Occupational Medicine, UMDNJ-Robert Wood Johnson Medical School, 170 Frelinghuysen Rd., Piscataway, NJ 08854. Tel.: 732-445-0176; Fax: 732-445-0119; E-mail: jlaskin@eohsi.rutgers.edu.

[2] The abbreviations used are: ROI, reactive oxygen intermediates; DPI, diphenyleneiodonium; NAME, nitroarginine methyl ester; MLE-15, murine lung epithelial cells; DTNB, 5,5′-dithiobis(2-nitrobenzoic acid); ATM, sodium aurothiomalate; CHO, Chinese hamster ovary; HPLC, high performance liquid chromatography.

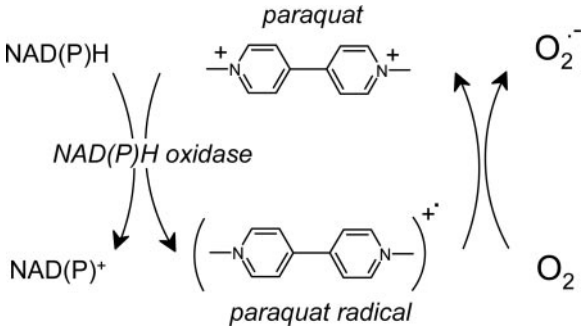

REACTION 1

enzyme known to reduce thioredoxin as well as a number of other oxidants, was identified as the active enzyme (23–28). Paraquat has been reported to accumulate in type II alveolar epithelial cells via an active transport system (29). Selective lung toxicity may be the result of coupling of this transport system with the redox cycling of paraquat by thioredoxin reductase.

MATERIALS AND METHODS

Chemicals and Reagents—10-Acetyl-3,7-dihydroxyphenoxazine (AMPLEX-RED) and 3H-phenoxazine (resorufin) were obtained from Molecular Probes (Eugene, OR). Rat cytochrome P450 reductase (Supersomes™, catalog no. 456514) was from BD Biosciences. Polyclonal antibodies to rat cytochrome P450 reductase (whole rabbit serum, catalog no. OSA-300) were from Stressgen (Victoria, BC). Paraquat, NADPH, NADH, horseradish peroxidase, 2′,5′-ADP-agarose, and all other reagents were purchased from Sigma-Aldrich. The Superose 12 HR 10/30 size exclusion column was obtained from Amersham Biosciences. Rat liver thioredoxin reductase was obtained from Cayman Chemical (Ann Arbor, MI).

Cells and Treatments—MLE-15 murine lung epithelial cells were kindly provided by Dr. Jacob Finkelstein (University of Rochester) (30). Parental CHO cells were obtained from the American Type Culture Collection (Manassas, VA). The preparation of CHO cells expressing cytochrome P450 reductase or control empty vector has been described previously (31). Cells were maintained in Dulbecco's modified Eagle's medium supplemented with 10% fetal bovine serum, penicillin (100 units/ml), and streptomycin (100 μg/ml) at 37 °C in 5% CO_2 in a humidified incubator. Tissue culture reagents were from Invitrogen. For recordings, cells were plated at varying densities ($0.05–0.5 \times 10^5$ cells) onto 35-mm plastic Petri dishes in phenol red-free Dulbecco's modified Eagle's medium with 10% fetal calf serum. At low density cells grow individually, whereas at higher densities cells grow as confluent monolayers. Recordings were performed in phosphate-buffered saline. Paraquat and other reagents were added sequentially directly to the medium. Recordings were suspended during the 10–15 s required to apply the drugs. Time was recorded continuously during the addition of reagents.

Self-referencing Electrodes—The preparation and characterization of the oxygen microsensors has been described previously (32–35). Microsensors were used in a self-referencing format to obtain a directional flux of oxygen by individual cells and monolayers, which is detected as a difference in current (Δfemptoamperes). The advantage of this method is that it minimizes noise and random drift in the measurements, factors that limit the use of standard oxygen electrodes (33).

Enzyme Assays—NAD(P)H:paraquat oxidoreductase activity was assayed in cell lysates by quantifying ROI generated via redox cycling of paraquat (36–38), by the paraquat-dependent consumption of oxygen or NADPH in the enzyme assay (39), and by the NADPH-dependent formation of paraquat radical (36, 37, 40). To prepare cell lysates for the assays, cells were gently scraped from the culture dishes, resuspended in phosphate-buffered saline, and sonicated on ice with three 15-s bursts and 1 min of cooling on ice between each sonication burst. Disrupted cells were centrifuged ($3000 \times g$, 10 min) to remove cellular debris, and the supernatants were either assayed immediately for enzyme activity or further used to purify and characterize the paraquat reductase (see further below). Unless otherwise specified, standard reaction mixes contained 50 mM phosphate buffer, pH 7.4, 0.5 mM NADPH or NADH, 10–100 μg of cell lysate protein, and 1–1000 μM paraquat in 0.1 ml. All enzyme assays were run at 37 °C.

Hydrogen peroxide production was assayed in 100-μl reaction mixes supplemented with 25 μM 10-acetyl-3,7-dihydroxyphenoxazine and 0.1 units/sample of horseradish peroxidase as previously described (41). The fluorescent product resorufin was quantified using an HTS 7000 Plus Bio Assay Reader (PerkinElmer Life Sciences) fitted with a 540-nm excitation filter and a 595-nm emission filter. Kinetic assays were performed in the presence of increasing concentrations of paraquat, and fluorescence of resorufin was measured every 2.5 min for 30 min. The rate of hydrogen peroxide formation was calculated based on a standard curve generated with hydrogen peroxide in a concentration range of 0.5–30 μM. Initial velocity studies of the NAD(P)H oxidase activity were performed as described previously (42). In some experiments purified rat liver thioredoxin reductase (5 units/ml) or recombinant enzyme (9.8 units/ml) was added in place of cell lysates.

Superoxide anion production was assayed by its ability to oxidize hydroethidine to 2-hydroxyethidium cation in the reaction mix; the product was detected using HPLC with fluorescence detection as described by Zhao *et al.* (43) with minor modifications in the chromatography protocol. HPLC was carried out using a Luna C18 (2), 3 μm, 250 × 2.0-mm column (Phenomenex, Torrance, CA) and a C18 guard column using a 0.2 ml/min flow rate. The column was equilibrated with 10% CH_3CN in 0.1% trifluoroacetic acid. The formed products were separated by a linear increase in CH_3CN concentration from 10 to 40% starting from 10 to 45 min. The signals from the detector were recorded and analyzed by CLASS-VP software (Shimadzu Scientific Instruments, Columbia, MD). Hydroxyl radicals were measured by the formation of 2-hydroxyterephthalate from terephthalate using HPLC with fluorescence detection (excitation 315 nm, emission 425 nm) as described by Mishin and Thomas (44).

The generation of paraquat radicals and depletion of NADPH in reaction mixtures were quantified in 0.5-ml cuvettes using a Lambda 20 UV/visible spectrophotometer

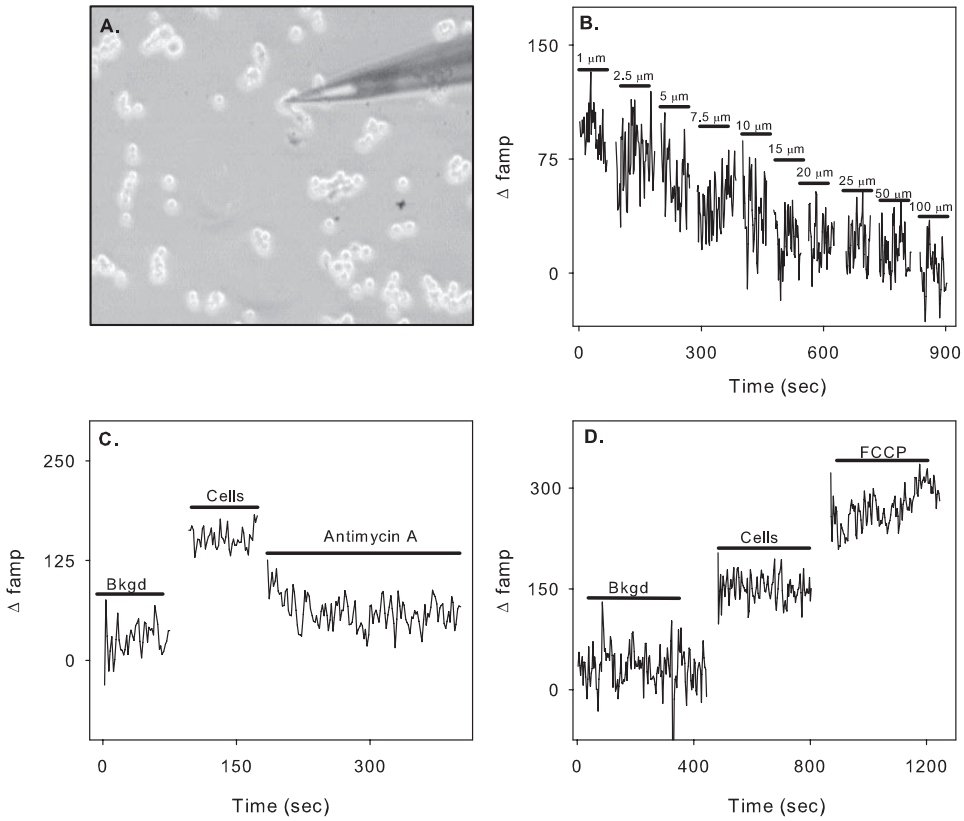

FIGURE 1. **Oxygen flux near surface membranes of lung epithelial cells.** *Panel A*, micrograph showing self-referencing oxygen microsensor placed near an MLE-15 cell. *Panel B*, oxygen flux measured at increasing distances from the cell membrane. Note that oxygen gradients were detected at distances of up to 25–50 μm from the cells. *Panel C*, effects of antimycin A on oxygen flux in lung epithelial cells. Initially recordings were obtained by placing the oxygen microsensor in the culture medium 1 mm above an MLE-15 cell. After obtaining a stable background (*Bkgd*) the probe was placed within 5 μm of the cell to obtain a recording of oxygen flux. After an additional 3 min, antimycin A (1 μg/ml, final concentration) was added to the culture medium. *Panel D*, effects of carbonyl cyanide *p*-trifluoromethoxyphenylhydrazone (*FCCP*; 1 μM) on oxygen flux into lung epithelial cells.

(PerkinElmer Life Sciences) scanning at 1 nm/s, recording at 1-nm intervals, and repeating the scan at 2.5-min intervals for 30 min. Paraquat radicals were quantified by increases in absorbance at 603 nm ($\epsilon_{603} = 1.20 \times 10^4$) (45). Because paraquat radicals are sensitive to oxygen (46), experiments were run in filled cuvettes covered tightly with Parafilm. NADPH depletion was measured by decreases in absorbance at 340 nm (39). A polarographic system fitted with a Clark oxygen electrode (Yellow Springs Instruments, Yellow Springs, OH) was used to characterize oxygen utilization during enzymatic redox cycling of paraquat.

Purification Studies—Lysates containing enzyme activity were centrifuged in an Eppendorf 5417R high speed centrifuge at 12,000 × *g* for 10 min to sediment membrane and mitochondrial fractions. The resulting supernatant was centrifuged in a Beckman L7–55 ultracentrifuge at 100,000 × *g* for 1 h, and the microsomal and post-microsomal supernatant fractions were collected. Approximately 40% of the paraquat oxidoreductase activity was contained in the post-microsomal supernatant fractions, whereas the remaining activity was present in membrane and microsomal fractions. The post-mitochondrial supernatant fractions were further purified by NADPH affinity chromatography as described by Wolff *et al.* (47). Briefly, 2′,5′-ADP-agarose was added (0.2 volume of settled resin per volume of post-microsomal supernatant), and the suspension was rocked in a cold room for 1 h and then centrifuged at 2000 × *g* for 5 min. The supernatant was discarded, and the resin was washed five times with phosphate-buffered saline containing 0.1% Nonidet P-40. The resin was then washed with phosphate-buffered saline containing 0.1% Nonidet P-40 and 5 mM NADPH. The NADPH eluate was concentrated using an Amicon Ultra centrifugal filter (Millipore, Billerica, MA) and then fractionated by size exclusion chromatography on a Superose 12 HR 10/30 column (GE Healthcare) in phosphate-buffered saline containing 0.1% Nonidet P-40, pH 7.4, at a flow rate of 0.3 ml/min. Absorbance of effluent fractions was monitored at 280 nm. The column was previously calibrated with Bio-Rad gel filtration standard proteins (thyroglobulin, M_r 60,000; bovine globulin, M_r 158,000; chicken ovalbumin, M_r 44,000). Fractions containing enzyme activity were analyzed on 10% SDS-polyacrylamide gels. Sequence analysis of protein bands in the gels were performed as previously described (48) and analyzed using NCBI Blast algorithms.

Thioredoxin Reductase Assay—Thioredoxin reductase activity of the purified paraquat reductase or the recombinant enzyme was assayed by the reduction of 5,5′-dithiobis(2-nitrobenzoic acid) (DTNB) in the presence of NADPH as described by Kang *et al.* (49). The assay mixture contained 0.2 M phosphate buffer, pH 7.4, 1 mM EDTA, 0.25 mM NADPH, 1 mM DTNB, and appropriate concentrations of purified recombinant thioredoxin reductase or lung cell extract. Enzyme activity was followed by increases in absorbance at 412 nm. In some experiments, 100 μM 1-chloro-2,4-dinitrobenzene or sodium aurothiomalate (ATM), inhibitors of mammalian thioredoxin reductase, were added the reaction mix.

Purification of Thioredoxin Reductase—A construct containing human cytosolic thioredoxin reductase (hTR1) in which the TGA (Sec) codon was replaced with the TGC codon (Sec498Cys) cloned into the PET 28a+ vector (Novagen) was kindly provided by Anton Turanov (University of Nebraska). The thioredoxin reductase was purified from *E. coli* (BL21(DE3), Novagen) transformed with the construct and induced to express the enzyme as previously described (50). Purity of the enzyme was confirmed by fractionation of the purified protein on a 10% SDS-polyacrylamide gel followed by Coomassie staining. Enzymatic activity was confirmed by measuring the enzymatic reduction of

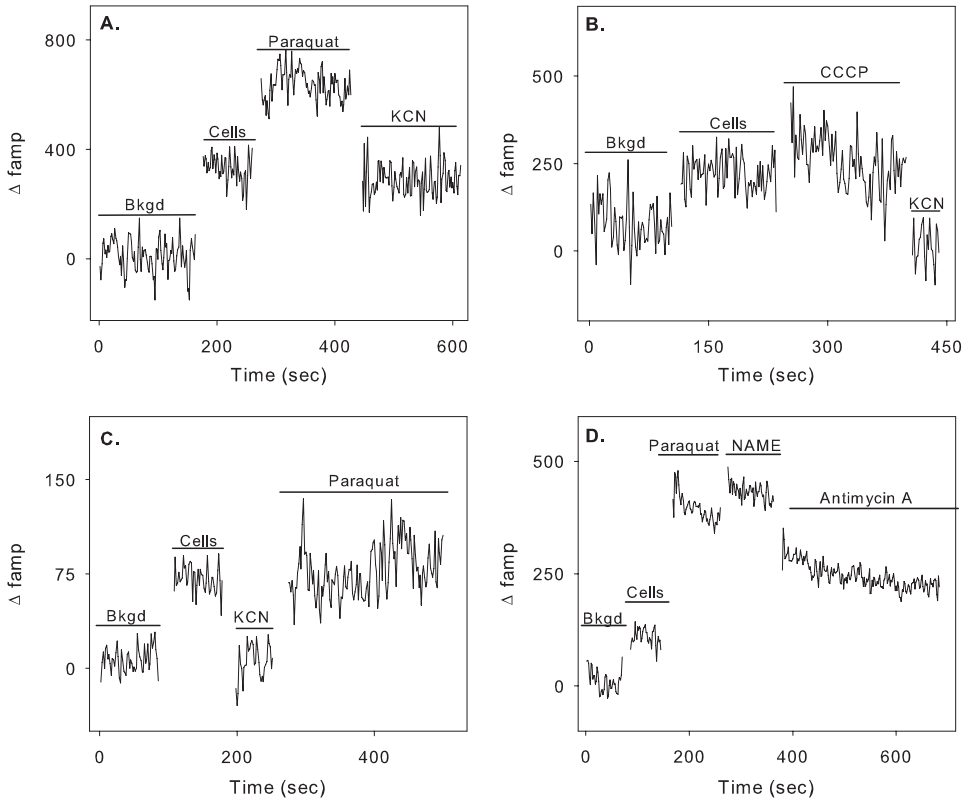

FIGURE 2. **Paraquat stimulates cellular oxygen flux.** *Panel A*, oxygen flux into lung cells was measured after treatment with paraquat (100 μM) followed by KCN (5 mM). *Panel B*, cells were treated with the proton ionophore carbonyl cyanide *m*-chlorophenylhydrazone (*CCCP*; 1 μM) followed by KCN. *Panel C*, oxygen flux was measured in paraquat-treated cells pretreated with KCN. *Panel D*, the sensitivity of paraquat-stimulated oxygen flux to NAME (5 mM) and antimycin A (1 μg/ml). *Bkgd*, background.

DTNB and inhibition of enzyme activity with 1-chloro-2,4-dinitrobenzene or ATM (51, 52).

RESULTS

Characterization of Lung Epithelial Cell Oxygen Flux—In initial experiments we used the polarographic self-referencing microsensor to characterize oxygen utilization by lung epithelial cells. When the sensor was placed 1–5 μm from the cells, an oxygen gradient could readily be detected (Figs. 1, *A* and *B*). By moving the probe away from the cells, the gradient was mapped. Oxygen flux was detectable at distances up to 50 μm from individual cells and 400–500 μm from confluent monolayers (Fig. 1*B* and not shown). The fact that oxygen gradients could be detected in areas surrounding the cells indicates that oxygen consumption by the cells is greater than the amount of oxygen available by its diffusion through the medium to the cells.

Treatment of the cells with mitochondrial electron transport chain inhibitors rotenone (complex I), antimycin A (complex III), or potassium cyanide (complex IV) markedly reduced the oxygen gradients surrounding the cells, indicating that the oxygen consumption was mainly mediated by mitochondrial respiration (Figs. 1, *panel C*, and 2 and not shown). This conclusion is supported by our findings that the mitochondrial protonophore uncouplers, carbonyl cyanide *p*-trifluoromethoxyphenylhydrazone and carbonyl cyanide *m*-chlorophenylhydrazone, enhanced oxygen uptake by the cells (Figs. 1*D* and 2*B*).

In further experiments we examined the effects of paraquat on oxygen flux into lung cells. The addition of 100 μM paraquat to the cells resulted in a marked increase (2–4-fold) in oxygen flux that was evident within 15–30 s and persisted for at least 30 min (Fig. 2*A*); smaller increases in oxygen flux (~1.5-fold) were observed with 10 μM paraquat (not shown). Neither antimycin A nor potassium cyanide, which block mitochondrial respiration, altered paraquat-induced oxygen flux (Figs. 2, *panels A* and *D*, and 3). These data indicate that the effects of paraquat are independent of mitochondrial respiration. Pretreatment of lung cells with inhibitors of mitochondrial respiration also had no effect on paraquat-induced oxygen flux (Fig. 2*C* and not shown). In contrast, carbonyl cyanide *p*-trifluoromethoxyphenylhydrazone and carbonyl cyanide *m*-chlorophenylhydrazone-induced increases in oxygen flux were completely blocked by potassium cyanide, demonstrating that the actions of the mitochondrial protonophores and paraquat are distinct (Fig. 2*B* and not shown).

Paraquat has also been reported to stimulate the diaphorase activity of nitric-oxide synthase, a process inhibited by the nitric-oxide synthase inhibitor nitroarginine methyl ester (NAME) (2). We found that treatment of the lung epithelial cells with NAME had no effect on mitochondrial or paraquat-induced oxygen flux (Fig. 2*D* and not shown). These data suggest that nitric-oxide synthase does not affect paraquat-induced oxygen uptake.

It is well recognized that several NADPH oxidases, including cytochrome P450 reductase, contribute to extra-mitochondrial oxygen utilization (53, 54). Paraquat is known to redox cycle via cytochrome P450 reductase; whether it is a substrate for NADPH oxidase is unknown (6). We found that diphenyleneiodonium (DPI), a non-selective inhibitor of FAD-dependent enzymes, including NADPH oxidase, readily blocked paraquat-induced oxygen flux into the cells without affecting mitochondrial respiration (Fig. 4*A*). This effect was independent of the order of addition of paraquat and DPI to the cultures (compare Figs. 4, *A* and *B*). Taken together, these data indicate that paraquat-induced alterations in oxygen uptake are dependent on an FAD-containing oxidoreductase activity in the cells.

To eliminate the possibility that cytochrome P450 reductase was responsible for paraquat-induced increases in oxygen flux, we analyzed the effects of the herbicide in cells overexpressing the enzyme. For these studies we used CHO cells stably transfected with mouse CYP450 reductase that have 35-fold more

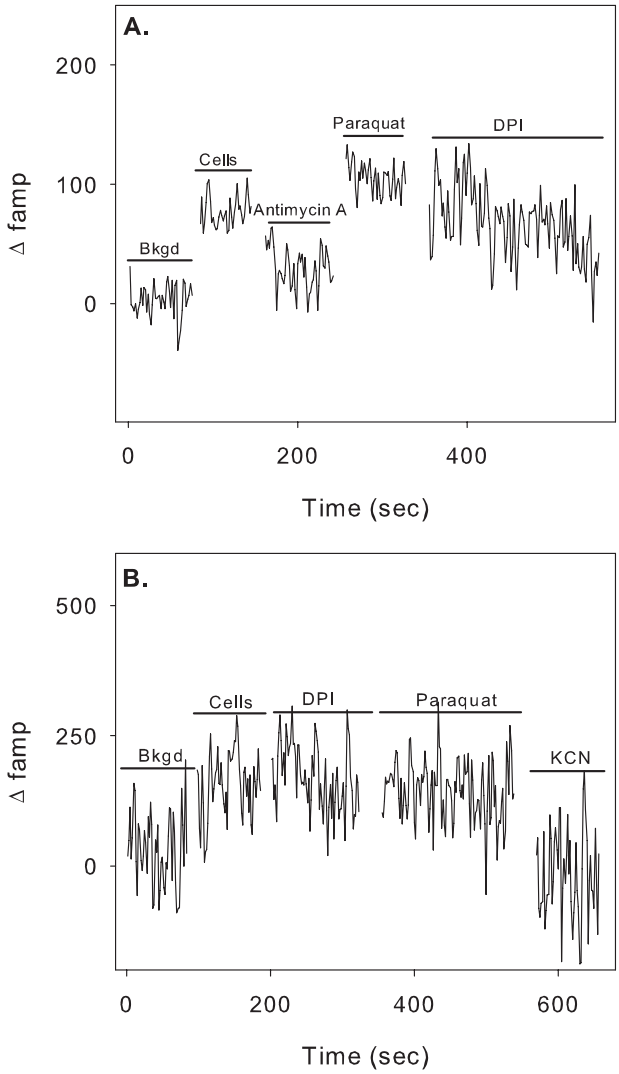

FIGURE 3. **Inhibition of paraquat-stimulated oxygen flux by DPI.** MLE-15 cells were treated with antimycin A (1 μg/ml), paraquat (100 μM), DPI (10 μM), or KCN (5 mM) as indicated in the figures. Oxygen flux was measured as described in Fig. 1. *Bkgd*, background.

enzyme activity when compared with wild type control CHO cells (31).[3] As observed with lung epithelial cells, paraquat caused a similar increase in oxygen flux into both wild type and cytochrome P450 reductase-overexpressing cells. Subsequent treatment of the cells with potassium cyanide reduced oxygen flux due to mitochondrial respiration (Fig. 5, *panels A* and *B*). The fact that the different cell types responded similarly to paraquat indicates that oxygen uptake by the cells induced by paraquat was independent of cytochrome P450 reductase activity.

Effects of Paraquat on Lung Epithelial Cell NADPH Oxidase—NADPH oxidase catalyzes the transfer of electrons from NADPH to oxygen resulting in the formation of superoxide anion. Superoxide anion rapidly dismutates into hydrogen peroxide and, in the presence of redox active metals, is a source of cytotoxic hydroxyl radicals (for review, see Refs. 10 and 11). NADPH oxidase enzyme activity can readily be quantified by the NADPH-dependent consumption of oxygen, utilization of NADPH, and the production of ROI due to redox cycling of paraquat (36–39). Mitochondria-free lysates prepared from lung epithelial cells contained very low levels of NADPH oxidase enzyme activity, as measured by oxygen consumption using a Clark oxygen electrode (Fig. 5). The addition of paraquat to the reaction mix caused a marked increase in enzyme activity that was dependent on NADPH. Oxygen consumption by this enzyme was inhibited by DPI (Fig. 5). These findings are consistent with our microsensor studies in intact cells and support the concept that the actions of paraquat are mediated by an FAD-containing NADPH oxidase.

In further studies we characterized the paraquat-stimulated NADPH oxidase activity in lung cell lysates. A one-electron reduction of paraquat by this enzyme would be expected to generate the paraquat radical (see Reaction 1). This radical is stable at low oxygen tension and can be quantified spectrophotometrically by its absorption maximum at 603 nm (45). Using sealed cuvettes to facilitate depletion of oxygen by the enzyme, reduced paraquat was found to readily accumulate with time in the reaction mixture in an NADPH-dependent reaction (Fig. 6*A*). When the cuvettes were re-oxygenated, the paraquat radical was oxidized back to paraquat, thus confirming the redox cycling reaction (data not shown). Paraquat also stimulates NADPH consumption in lung cell lysates. In the absence of paraquat cell lysates were found to metabolize relatively low basal levels of NADPH (Fig. 6*C*). The addition of paraquat to the reaction mix caused a marked increase in NADPH metabolism (Fig. 6*D*). Both paraquat radical formation and NADPH metabolism were inhibited by DPI (Fig. 6, *panels B* and *E*).

We next determined if the NADPH oxidase activity in lung cell lysates could generate ROI in response to paraquat. For these studies the formation of hydrogen peroxide, superoxide anion and hydroxyl radicals was analyzed. In the absence of paraquat, only low basal levels of hydrogen peroxide were observed; a small increase in activity was noted when either NADPH or NADH was added to the assay mix (Fig. 7, *panels A* and *B*). The addition of paraquat to the reaction resulted in a marked increase in enzymatic activity with both cofactors. Approximately four times more activity was evident with NADPH when compared with NADH (Figs. 7, *panels A* and *B*). The effects of paraquat on hydrogen peroxide production were concentration- and time-dependent; maximal activity was observed with 100 μM paraquat (Fig. 7*C*). The accumulation of hydrogen peroxide was abolished by catalase (10 units/ml) but not superoxide dismutase (400 units/ml), confirming that hydrogen peroxide was formed in the assay (data not shown). Increased activity of paraquat in the presence of NADPH when compared with NADH was due to a lower half-maximal activating concentration (K_{act}) and increased V_{max} for paraquat. Thus, the K_{act} for paraquat was 41.5 μM with NADPH and 680.5 μM for NADH. The V_{max} for enzyme activity with paraquat was 108 nmol of H_2O_2/min/mg of protein and 226 nmol of H_2O_2/min/mg of protein with NADH and NADPH, respectively (Table 1). In the presence of 100 μM paraquat, there was a marked increase in the V_{max} value for NADH and NADPH, with only small changes in the K_m values for these cofactors

[3] J. P. Gray, D. E. Heck, V. Mishin, P. J. S. Smith, J.-Y. Hong, M. Thiruchelvam, D. A. Cory-Slechta, D. L. Laskin, and Jeffrey D. Laskin, unpublished information.

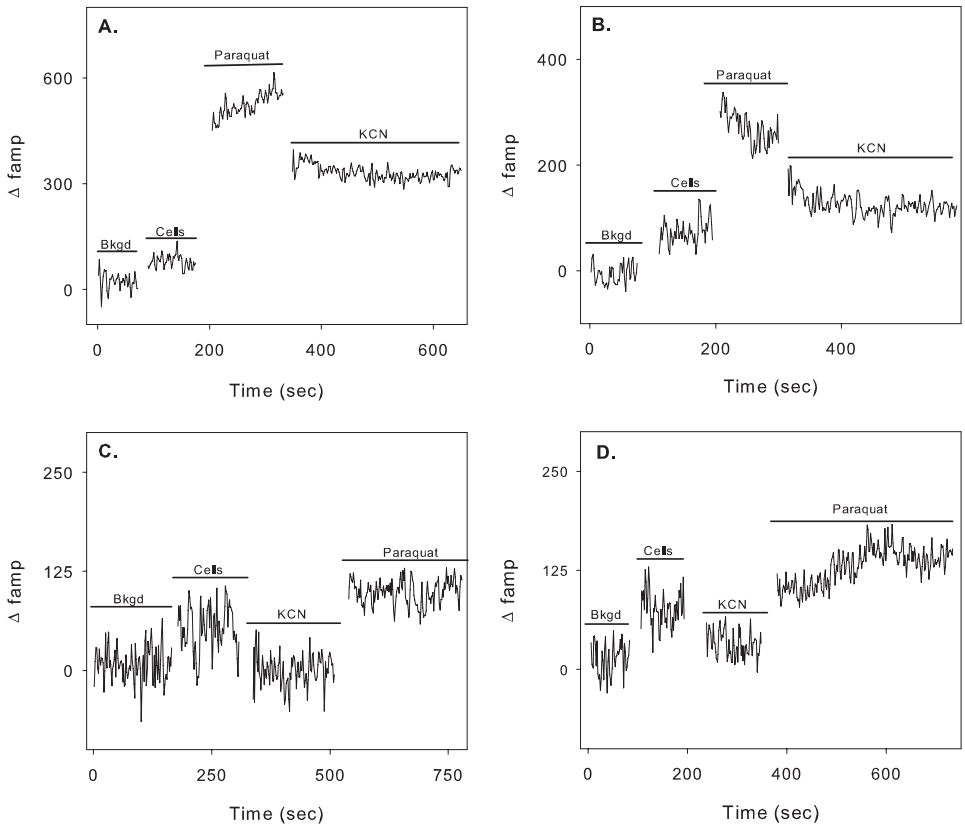

FIGURE 4. **Paraquat-stimulated oxygen flux in wild type CHO cells and CHO cells overexpressing cytochrome P450 reductase.** *Panel A*, paraquat-stimulated oxygen flux in wild type CHO cells. Cells were treated with paraquat (100 μM) followed by KCN (5 mM). *Panel B*, paraquat-stimulated oxygen flux in CHO cells overexpressing cytochrome P450 reductase. *Panels C* and *D*, KCN pretreatment does not prevent paraquat-induced alterations in oxygen flux in wild type CHO cells or CHO cells overexpressing cytochrome P450 reductase, respectively. *Bkgd*, background.

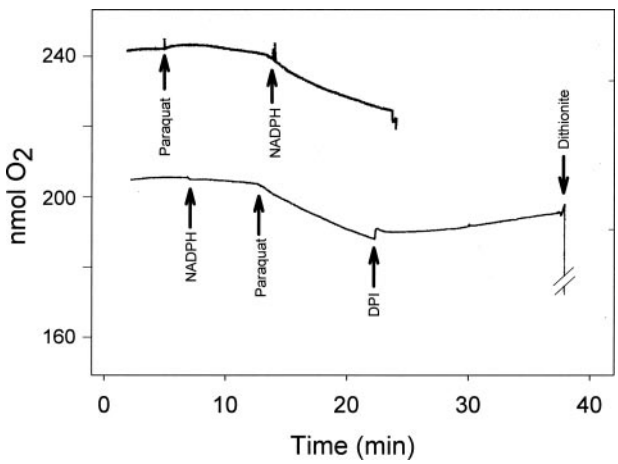

FIGURE 5. **Paraquat stimulates NADPH-dependent oxygen consumption by lung epithelial cell lysates.** A Clark oxygen electrode was used to quantify oxygen utilization by lung cell lysates as described under "Materials and Methods." After establishing a base line, paraquat (100 μM) and NADPH (0.5 mM) were added in the order indicated by the *arrows*. Note the marked increase in oxygen consumption when both paraquat and NADPH were added. The addition of DPI (10 μM) inhibited oxygen consumption (*lower curve*). At the end of the experiment several grains of sodium dithionite were added to deplete remaining oxygen for calibration (shown by the *arrow* on the *lower curve*, not to scale).

(Table 2). The increase in V_{max} for NADPH was ~5-fold greater than for NADH, thus accounting for differences in activity of the lysates with these pyridine nucleotides.

Paraquat was also found to stimulate production of superoxide anion and hydroxyl radicals (Fig. 7, *panels D–F*). The accumulation of these ROI was dependent on NADPH; superoxide anion detection was inhibitable by superoxide dismutase but not by catalase (data not shown). Hydroxyl radical production was supported by the presence of redox-active iron. In the absence of iron only very low levels of hydroxyl radicals were formed (Fig. 7*E*). These findings indicate that hydroxyl radicals are derived from hydrogen peroxide via the Fenton reaction (55). Hydroxyl radical production was prevented by catalase and the hydroxyl radical scavenger dimethyl sulfoxide (Ref. 44 and data not shown). The fact that low levels of hydroxyl radical were detected in the absence of added iron may be due to the presence of traces of redox active transition metals in the cell lysates.

We also found that paraquat-induced NADPH oxidase activity was suppressed by DPI; the IC_{50} for this inhibitor was 1 μM (Fig. 7*G*). In contrast, enzyme activity was unaffected by the nitric-oxide synthase inhibitor, NAME or the NADPH-quinone reductase inhibitors, dicoumarol or chrysin (5,7-dihydroxyflavone), indicating that these enzymes do not mediate paraquat NAD(P)H oxidoreductase activity (Fig. 7*G* and not shown). Although cDNA-expressed rat cytochrome P450 reductase was inhibited by a polyclonal antibody to this enzyme, this antibody did not block lung epithelial cell paraquat NAD(P)H oxidoreductase activity (Fig. 7*H*). These data provide additional evidence that the effects of paraquat are not dependent on cytochrome P450 reductase.

We next characterized the lung epithelial cell paraquat NAD(P)H oxidoreductase activity. As indicated under "Material and Methods," ~40% of the activity was identified in post-microsomal supernatant fractions of the cells. Enzyme activity in this fraction was purified by 2′,5′-ADP-agarose affinity and Superose size exclusion chromatography. Two peaks with approximate molecular weights of 100 and 50 were identified. When analyzed by SDS-polyacrylamide gel electrophoresis, the first peak contained two proteins (M_r 58,000 and 39,000), whereas the second peak contained a single M_r 58,000 protein (not shown). Based on sequence analysis, the M_r 58,000 protein was identified as thioredoxin reductase (M_r 57,000 (56)). The identity of the lower molecular weight band was not determined. To confirm the identity of the paraquat reductase in the cytosolic fraction of the lung epithelial cells, we next assayed the 50-kDa fraction for

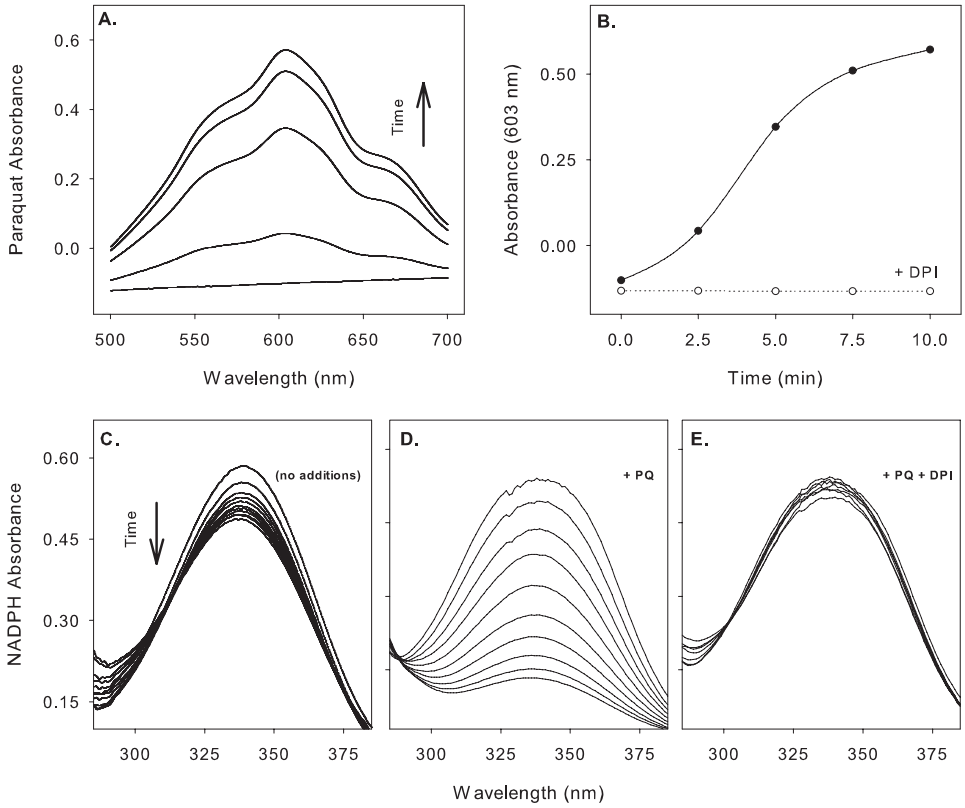

FIGURE 6. **Reduction of paraquat and paraquat-stimulated NADPH metabolism by lung epithelial cell lysates.** Reaction mixtures containing paraquat (100 μM), NADPH (0.1 mM), and cell lysates were analyzed in 0.5 ml spectrophotometer cuvettes at 37 °C. Absorbance spectra were recorded at 2.5 min intervals. *Panel A*, time-dependent increase in the production of the blue/violet paraquat radical (λ_{max} = 603 nm). To measure paraquat radical reaction mixtures were preincubated for 30 min in sealed cuvettes before analysis. *Panel B*, inhibitory effects of DPI (10 μM) on paraquat radical formation. Data are presented as changes in absorbance at 603 nm over time. *Panel C*, basal metabolism of NADPH in cell lysates in the absence of paraquat. Reactions were run in unsealed cuvettes. *Panel D*, paraquat (*PQ*)-stimulated NADPH metabolism. Paraquat was added directly to the cuvette and then analyzed. *Panel E*, inhibition of paraquat-stimulated NADPH metabolism by DPI. DPI (10 μM) and paraquat were added to the cuvette and then analyzed.

thioredoxin reductase activity. We found that this fraction readily reduced DTNB, which was inhibited by DPI and the thioredoxin reductase inhibitors 1-chloro-2,4-dinitrobenzene and sodium aurothiomalate (51, 52) (Fig. 8*A* and not shown). These data indicate that the paraquat redox active material purified from lung epithelial cells was thioredoxin reductase.

To confirm the reactivity of thioredoxin reductase with paraquat, we next analyzed its activity using recombinant thioredoxin reductase or purified rat liver enzyme. In the presence of NADPH, these enzymes generated low levels of hydrogen peroxide; this reaction was markedly increased by paraquat (Fig. 8*B*). Both recombinant thioredoxin reductase and the rat liver enzyme also generated paraquat radical in the absence of molecular oxygen in an NADPH-dependent reaction (Fig. 8*C* and not shown). Furthermore, using a Clark oxygen electrode, paraquat was shown to stimulate oxygen utilization by the recombinant thioredoxin reductase (Fig. 8*D*). Oxygen utilization was inhibited by DPI. Taken together, these data demonstrate that thioredoxin reductase is an important component of the cellular redox cycling of paraquat.

DISCUSSION

Of fundamental importance to the survival of mammalian cells is the availability of molecular oxygen. Although largely used in mitochondrial respiration, cells also consume oxygen in numerous extra-mitochondrial enzymatic and non-enzymatic processes (53, 54). Indeed it has been estimated that in healthy respiring tissues non-mitochondrial respiration accounts for ~6–14% of oxygen consumption (54). Redox cycling has been recognized as one important pathway by which cells can utilize oxygen to generate reactive oxygen species (46). Many endogenous cellular components have the capacity to participate in redox reactions, most notably, transition metals and a variety of single electron donating enzymes (36–38). Redox cycling is also thought to mediate the action of many toxicants including paraquat (20).

Paraquat is unusually toxic to the lung, presumably due to its selective uptake by lung cells and localized redox cycling in the alveolar epithelium (57, 58). The present studies demonstrate that micromolar concentrations of paraquat increase cellular oxygen consumption by lung epithelial cells. This activity was not inhibited by cyanide or antimycin A, indicating that the actions of paraquat were not dependent on mitochondrial respiration. These data are consistent with redox cycling of paraquat (14, 17). Increases in oxygen utilization by paraquat in lung epithelial cells were inhibited by DPI, indicating that redox cycling occurs via an FAD-dependent enzyme. However, DPI did not alter cellular respiration, supporting the idea that the effects of paraquat are independent of mitochondria functioning.

In our studies a highly sensitive oxygen microsensor was used to quantify the effects of paraquat on oxygen uptake by lung epithelial cells (33–35, 59). Of interest was our finding that a significant gradient of oxygen is generated around actively respiring cells. Thus, the availability of oxygen in the cell culture medium may limit metabolic activity. In paraquat-treated cells, a steeper gradient was observed surrounding the cells. This is consistent with the idea that additional oxygen is utilized during redox cycling, potentially limiting the amount of oxygen available for respiration. This could result in increased oxidative stress, leading to dysregulation of gene expression, altered energy reserves, and toxicity (60, 61). Similar actions may also occur in bacteria where

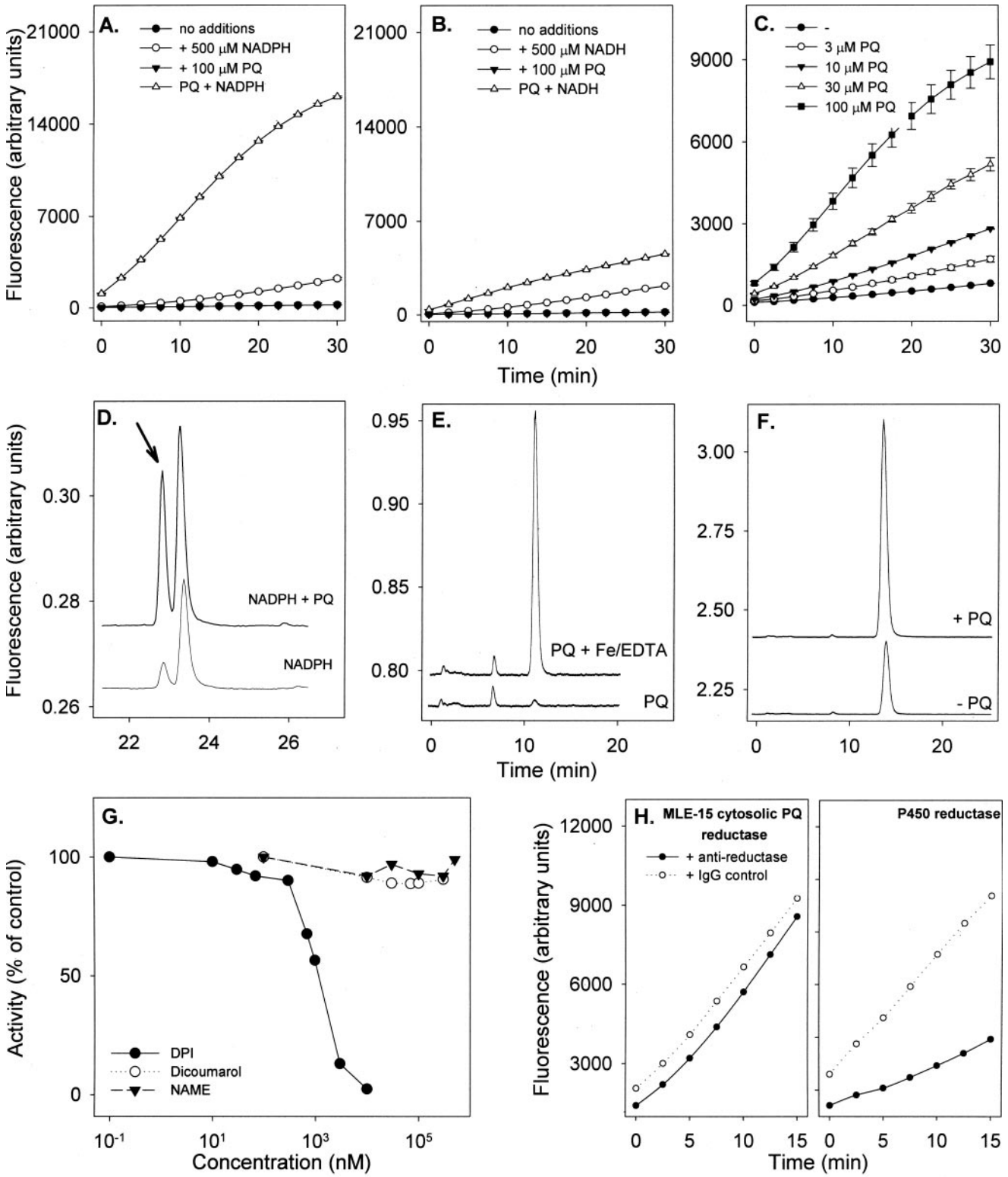

FIGURE 7. **Paraquat redox cycling stimulates ROI production in lung epithelial cell lysates.** *Panels A* and *B*, effects of NADPH or NADH, respectively, on the formation of hydrogen peroxide as assayed using 10-acetyl-3,7-dihydroxyphenoxazine (AMPLEX-RED) (82). *PQ*, paraquat. *Panel C*, increasing concentrations of paraquat stimulate hydrogen peroxide production. Reaction mixes contained 500 μM NADPH. *Panel D*, redox cycling of paraquat generates superoxide anion. Superoxide anion was assayed in reaction mixes after 45 min by the formation of 2-hydroethidium cation (indicated by the *arrow*) in the absence and presence of paraquat (100 μM). 2-Hydroethidine was separated from hydroethidine (second peak) by HPLC using fluorescence detection. *Panels E* and *F*, redox active iron is required for the formation of hydroxyl radicals by paraquat. Hydroxyl radicals were assayed in reaction mixes after 3 h of incubation by the formation of 2-hydroxyterephthalate from terephthalate using HPLC with fluorescence detection. In *panel E* reactions containing 100 μM paraquat were run in the absence and presence of 100 μM Fe^{+3}/EDTA. In *panel F* reactions containing Fe^{+3}/EDTA were run in the absence and presence of 1 mM paraquat. *Panel G*, effects of inhibitors on paraquat-stimulated NADPH oxidase activity. Paraquat-stimulated hydrogen peroxide formation was assayed after 30 min in reaction mixes containing NADPH and increasing concentrations of DPI, dicoumarol, or NAME. *Panel H*, effects of P450 reductase antibodies on redox cycling by paraquat. Reaction mixes containing cell lysates or recombinant P450 reductase were incubated without and with antibody to P450 reductase and then assayed for paraquat-stimulated hydrogen peroxide production.

Hassan and Fridovich (18) reported that paraquat-induced oxygen utilization in *E. coli* occurs directly at the expense of normal respiration.

TABLE 1

Activation kinetics for the production of ROI by paraquat in lung cell extracts

Treatments	K_{act}[a]	V_{max}
	μM	*nmol H_2O_2/min/mg of protein*
NADH	680.5	108
NADPH	41.5	226

[a] Initial reaction velocities for the production of hydrogen peroxide using increasing concentrations of paraquat were analyzed in standard reaction mixes supplemented with 500 μM NADPH or NADH.

TABLE 2

Effects of paraquat on reaction kinetics of NADH and NADPH in lung cell extracts

Treatments	K_m[a]	V_{max}
	μM	*nmol H_2O_2/min/mg of protein*
+NADH	9.7	23.1
+NADH + paraquat	12.8	57.4
+NADPH	5.9	12.7
+NADPH + paraquat	8.9	245

[a] Initial reaction velocities for the production of hydrogen peroxide using increasing concentrations of NADH or NADPH were analyzed in standard reaction mixes in the absence and presence of paraquat (100 μM).

Previous studies have suggested that paraquat-induced redox cycling occurs via cytochrome P450 reductase (3, 14, 62). In contrast, our findings demonstrate that cells overexpressing this enzyme do not display increased oxygen uptake when compared with non-overexpressing parental cells, indicating that cytochrome P450 reductase is not a major contributor to paraquat-induced changes in cellular oxygen flux. Thus, increased oxygen utilization in response to paraquat must be mediated by a distinct one electron reductase. In this regard the present studies demonstrate that murine lung epithelial cells contain a paraquat reductase activity that utilizes molecular oxygen to initiate paraquat redox cycling with resultant generation of ROI. This enzymatic activity, which is FAD- and NADH- or NADPH-dependent, readily catalyzes the generation of the characteristic blue-violet paraquat radical (see Reaction 1) and is distinct from cytochrome P450 reductase. Thus, in contrast to P450 enzyme, the paraquat reductase is present in cytosolic fractions of cells and is capable of utilizing NADH as a source of reducing equivalents. Moreover, the paraquat reductase is not inhibitable by antibodies to cytochrome P450 reductase. The molecular weight of purified paraquat reductase is significantly lower than cytochrome P450 reductase.

Under aerobic conditions the paraquat reductase activity in lung epithelial cells was directly associated with the NADPH-dependent utilization of dioxygen as paraquat radical recycled back to paraquat. Both superoxide anion and hydrogen peroxide were generated during the process. Interestingly, in the absence of redox active iron, only low amounts of hydroxyl radicals were formed. This was not unexpected since in mammalian cells hydroxyl radical is largely derived from hydrogen peroxide by the Fenton reaction (55). This reaction requires redox active transition metals which are in low abundance in mammalian cells. Thus, damage to lung epithelial cells by paraquat-generated hydroxyl radicals may be limited.

Identification of the NAD(P)H: paraquat oxidoreductase activity as thioredoxin reductase was accomplished after purification and sequence analysis. This was confirmed by demonstrating that the enzyme activity purified from lung epithelial cells contains thioredoxin reductase activity and that highly purified rat liver thioredoxin reductase and recombinant human thioredoxin reductase were able to redox cycle paraquat and to reduce paraquat to paraquat radical under anaerobic conditions. It should be

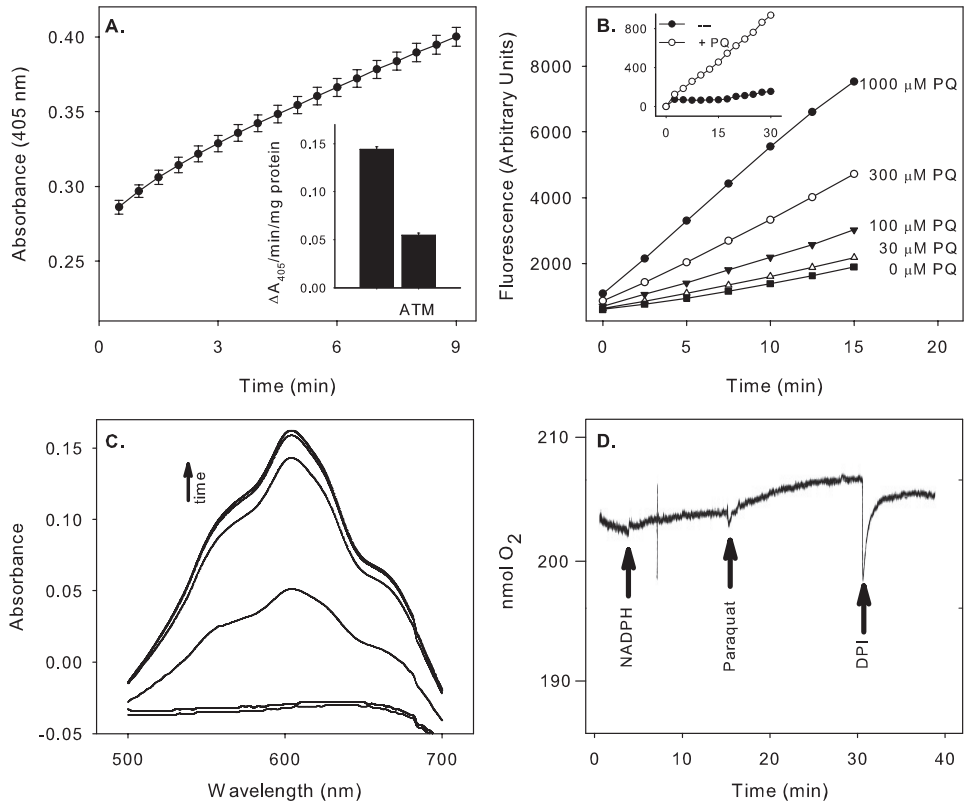

FIGURE 8. **Thioredoxin reductase activity of purified material from lung epithelial cells and characterization of paraquat redox cycling using recombinant thioredoxin reductase.** *Panel A*, thioredoxin reductase activity in material purified from lung epithelial cells was analyzed using DTNB as the substrate. The thioredoxin reductase inhibitor ATM (100 μM) inhibited DTNB reduction (*inset*). *Panel B*, ability of paraquat (*PQ*) to redox cycle using recombinant thioredoxin reductase or rat liver thioredoxin reductase (*inset*). Redox cycling was quantified using the AMPLEX-RED reaction. Reaction mixes contained 0.5 mM NADPH and increasing concentrations of paraquat (0–1000 μM; 1000 μM *inset*). *Panel C*, recombinant thioredoxin reductase catalyzes the formation of paraquat radical. Reaction mixes contained NADPH and paraquat (100 μM) and were run in sealed cuvettes as in the legend to Fig. 6. *Panel D*, paraquat stimulates oxygen utilization by recombinant thioredoxin reductase. Oxygen utilization was measured as indicated in the legend to Fig. 5. The *arrows* show the addition of 0.5 mM NADPH, 100 μM paraquat, and 10 μM DPI.

noted that, besides P450 reductase, additional paraquat reductases have been identified in both mammalian cells and in bacteria (18, 19, 36–38). Thus, Day *et al.* (2) reported that rat nitric-oxide synthase can reduce paraquat in a process inhibitable by nitric-oxide synthase inhibitors that prevent NADPH oxidation. In contrast, we found that the nitric-oxide synthase inhibitor NAME had no effect on paraquat redox cycling in our system, suggesting that the enzyme is not nitric-oxide synthase. The molecular weights for nitric-oxide synthase and paraquat reductase are also clearly distinct (63). In *E. coli* several paraquat reductases have been identified including NADPH:thioredoxin reductase, NADPH: ferredoxin reductase, and the ferredoxin-containing NADPH:sulfite reductase (64, 65). It is important to note that the thioredoxin reductases from mammals and *E. coli* are mechanistically and structurally distinct, making it difficult to compare activity between these two proteins (56).

In addition to increasing oxygen consumption, paraquat dramatically reduces cellular NADPH concentrations (66). Because NADPH is required in multiple biological pathways, including the reduction of oxidized glutathione, the function of cytochrome P450 enzymes, and many biosynthetic reactions, depletion of this pyridine nucleotide can inhibit many essential cellular functions and contribute to toxicity (67). Overstimulation of the glucose 6-phosphate shunt by accumulated NADP+ may also contribute to toxicity by diverting glucose from ATP production. This hypothesis is supported by findings that overexpression of glucose 6-phosphate dehydrogenase enhances paraquat toxicity in NIH-3T3 cells (68).

Attempts to ameliorate paraquat-induced lung toxicity have met with mixed success. Although anti-inflammatory corticosteroids are commonly administered, there is limited evidence that these compounds provide therapeutic benefits (69). Many compounds that reduce production of ROI, including antioxidants (*N*-acetylcysteine and glutathione), catechols and flavonoids (epigallocatechin gallate and apocynin), and metal chelators (desferoxamine), protect against paraquat toxicity in cell culture systems (70–75). However, these treatments have been less successful in various *in vivo* models, particularly when administered after, rather than before, paraquat exposure (76–78). Our data suggest that inhibition of thioredoxin reductase in cases of paraquat poisoning may ameliorate toxicity. Further studies are needed to identify therapeutic inhibitors of this enzyme in lung tissues.

In summary, the present studies show that paraquat increases cyanide-insensitive respiration in murine lung epithelial cells. Paraquat is known to function via redox cycling, and our findings that paraquat-stimulated respiration in lung cells was inhibited by DPI suggest that its actions are mediated by an FAD-dependent cellular oxidoreductase. Based on these findings we purified an NAD(P)H-dependent oxidoreductase from the cytoplasm of lung epithelial cells and demonstrated that it readily utilized oxygen and generated highly toxic reactive oxygen species. This activity was independent of cytochrome P450 reductase and identified as the FAD-containing enzyme thioredoxin reductase. Thioredoxin reductase is an essential enzyme for protection against oxidative stress (51, 79–81). Thus, it is surprising that it can also promote oxidative stress by redox cycling of paraquat. Further studies are required to characterize the mechanism by which paraquat activates thioredoxin reductase and to more precisely define its role in paraquat pneumotoxicity.

Acknowledgment—We thank Craig Hamilton for technical assistance with the self-referencing electrodes.

REFERENCES

1. Kimbrough, R. D., and Gaines, T. B. (1970) *Toxicol. Appl. Pharmacol.* **17,** 679–690
2. Day, B. J., Patel, M., Calavetta, L., Chang, L. Y., and Stamler, J. S. (1999) *Proc. Natl. Acad. Sci. U. S. A.* **96,** 12760–12765
3. Clejan, L. A., and Cederbaum, A. I. (1993) *Biochem. J.* **295,** 781–786
4. Michaelis, L., and Hill, E. S. (1933) *J. Am. Chem. Soc.* **55,** 1481–1494
5. Rashba-Step, J., and Cederbaum, A. I. (1994) *Mol. Pharmacol.* **45,** 150–157
6. Bonneh-Barkay, D., Reaney, S. H., Langston, W. J., and Di Monte, D. A. (2005) *Mol. Brain Res.* **134,** 52–56
7. Dicker, E., and Cederbaum, A. I. (1991) *Biochem. Pharmacol.* **42,** 529–535
8. Karakashev, P., Petrov, L., and Alexandrova, A. (2000) *Neoplasma* **47,** 122–124
9. Schweich, M. D., Lison, D., and Lauwerys, R. (1994) *Biochem. Pharmacol.* **47,** 1395–1400
10. McCord, J. M. (2000) *Am. J. Med.* **108,** 652–659
11. Mason, R. P. (1990) *Environ. Health Perspect.* **87,** 237–243
12. Kappus, H. (1986) *Biochem. Pharmacol.* **35,** 1–6
13. Prabhakar, N. R., and Kumar, G. K. (2004) *Biol. Chem.* **385,** 217–221
14. Gage, J. C. (1968) *Biochem. J.* **109,** 757–761
15. Rossouw, D. J., and Engelbrecht, F. M. (1979) *S. Afr. Med. J.* **55,** 558–560
16. Rossouw, D. J., and Engelbrecht, F. M. (1979) *S. Afr. Med. J.* **55,** 20–23
17. Rossouw, D. J., and Engelbrecht, F. M. (1978) *S. Afr. Med. J.* **54,** 1101–1104
18. Hassan, H. M., and Fridovich, I. (1977) *J. Biol. Chem.* **252,** 7667–7672
19. Hassan, H. M., and Fridovich, I. (1978) *J. Biol. Chem.* **253,** 8143–8148
20. Adam, A., Smith, L. L., and Cohen, G. M. (1990) *Environ. Health Perspect.* **85,** 113–117
21. Adam, A., Smith, L. L., and Cohen, G. M. (1990) *Biochem. Pharmacol.* **40,** 1533–1539
22. Rossouw, D. J., and Engelbrecht, F. M. (1978) *S. Afr. Med. J.* **54,** 199–201
23. Spyrou, G., and Holmgren, A. (1996) *Biochem. Biophys. Res. Commun.* **220,** 42–46
24. Karimpour, S., Lou, J., Lin, L. L., Rene, L. M., Lagunas, L., Ma, X., Karra, S., Bradbury, C. M., Markovina, S., Goswami, P. C., Spitz, D. R., Hirota, K., Kalvakolanu, D. V., Yodoi, J., and Gius, D. (2002) *Oncogene* **21,** 6317–6327
25. Holmgren, A., and Lyckeborg, C. (1980) *Proc. Natl. Acad. Sci. U. S. A.* **77,** 5149–5152
26. Ganther, H. E. (1999) *Carcinogenesis* **20,** 1657–1666
27. Gromer, S., and Gross, J. H. (2002) *J. Biol. Chem.* **277,** 9701–9706
28. Andersson, M., Holmgren, A., and Spyrou, G. (1996) *J. Biol. Chem.* **271,** 10116–10120
29. Waddell, W. J., and Marlowe, C. (1980) *Toxicol. Appl. Pharmacol.* **56,** 127–140
30. Barrett, E. G., Johnston, C., Oberdorster, G., and Finkelstein, J. N. (1998) *Am. J. Physiol.* **275,** L1110–L1119
31. Han, J. F., Wang, S. L., He, X. Y., Liu, C. Y., and Hong, J. Y. (2006) *Toxicol. Sci.* **91,** 42–48
32. Jung, S. K., Trimarchi, J. R., Sanger, R. H., and Smith, P. J. (2001) *Anal. Chem.* **73,** 3759–3767
33. Land, S. C., Porterfield, D. M., Sanger, R. H., and Smith, P. J. (1999) *J. Exp. Biol.* **202,** 211–218
34. Porterfield, D. M., Corkey, R. F., Sanger, R. H., Tornheim, K., Smith, P. J., and Corkey, B. E. (2000) *Diabetes* **49,** 1511–1516
35. Porterfield, D. M., Laskin, J. D., Jung, S. K., Malchow, R. P., Billack, B., Smith, P. J., and Heck, D. E. (2001) *Am. J. Physiol. Lung Cell. Mol. Physiol.* **281,** 904–912
36. Bus, J. S., Aust, S. D., and Gibson, J. E. (1974) *Biochem. Biophys. Res.*

Commun. **58,** 749–755
37. Winterbourn, C. C. (1981) *FEBS Lett.* **128,** 339–342
38. Tampo, Y., Tsukamoto, M., and Yonaha, M. (1999) *Free Radic Biol. Med.* **27,** 588–595
39. Zhang, Z., Yu, J., and Stanton, R. C. (2000) *Anal. Biochem.* **285,** 163–167
40. Weidauer, E., Morke, W., Foth, H., and Bromme, H. J. (2002) *Arch. Toxicol.* **76,** 89–95
41. Towne, V., Will, M., Oswald, B., and Zhao, Q. (2004) *Anal. Biochem.* **334,** 290–296
42. Vetrano, A. M., Heck, D. E., Mariano, T. M., Mishin, V., Laskin, D. L., and Laskin, J. D. (2005) *J. Biol. Chem.* **280,** 35372–35381
43. Zhao, H., Joseph, J., Fales, H. M., Sokoloski, E. A., Levine, R. L., Vasquez-Vivar, J., and Kalyanaraman, B. (2005) *Proc. Natl. Acad. Sci. U. S. A.* **102,** 5727–5732
44. Mishin, V. M., and Thomas, P. E. (2004) *Biochem. Pharmacol.* **68,** 747–752
45. Autor, A. P. (1977) *Biochemical Mechanisms of Paraquat Toxicity*, I[st] Ed., pp. 21–38, Academic Press, New York
46. Farrington, J. A., Ebert, M., Land, E. J., and Fletcher, K. (1973) *Biochim. Biophys. Acta* **314,** 372–381
47. Wolff, D. J., Lubeskie, A., and Li, C. (1997) *Arch. Biochem. Biophys.* **338,** 73–82
48. Senn, H., Eugster, A., Otting, G., Suter, F., and Wuthrich, K. (1987) *Eur. Biophys. J.* **14,** 301–306
49. Kang, H. J., Hong, S. M., Kim, B. C., Park, E. H., Ahn, K., and Lim, C. J. (2006) *Mol. Cell* **22,** 113–118
50. Turanov, A. A., Su, D., and Gladyshev, V. N. (2006) *J. Biol. Chem.* **281,** 22953–22963
51. Nordberg, J., and Arner, E. S. (2001) *Free Radic Biol. Med.* **31,** 1287–1312
52. Gromer, S., Arscott, L. D., Williams, C. H., Jr., Schirmer, R. H., and Becker, K. (1998) *J. Biol. Chem.* **273,** 20096–20101
53. Cadenas, E., and Davies, K. J. (2000) *Free Radic. Biol. Med.* **29,** 222–230
54. Mason, H. S. (1957) *Adv. Enzymol. Relat. Subj. Biochem.* **19,** 79–233
55. Fenton, H. J. H. (1876) *Chem. News* **33,** 190
56. Becker, K., Gromer, S., Schirmer, R. H., and Muller, S. (2000) *Eur. J. Biochem.* **267,** 6118–6125
57. Smith, L. L., Wyatt, I., and Cohen, G. M. (1982) *Biochem. Pharmacol.* **31,** 3029–3033
58. Rannels, D. E., Kameji, R., Pegg, A. E., and Rannels, S. R. (1989) *Am. J. Physiol.* **257,** L346–L353
59. Jung, S. K., Hammar, K., and Smith, P. J. (2000) *Biol. Bull* **199,** 197–198
60. Wenger, R. H., and Gassmann, M. (1997) *Biol. Chem.* **378,** 609–616
61. Pouyssegur, J., and Mechta-Grigoriou, F. (2006) *Biol. Chem.* **387,** 1337–1346
62. Clejan, L., and Cederbaum, A. I. (1989) *Biochem. Pharmacol.* **38,** 1779–1786
63. Bredt, D. S., and Snyder, S. H. (1990) *Proc. Natl. Acad. Sci. U. S. A.* **87,** 682–685
64. Liochev, S. I., Hausladen, A., Beyer, W. F., Jr., and Fridovich, I. (1994) *Proc. Natl. Acad. Sci. U. S. A.* **91,** 1328–1331
65. Gaudu, P., and Fontecave, M. (1994) *Eur. J. Biochem.* **226,** 459–463
66. Witschi, H., Kacew, S., Hirai, K. I., and Cote, M. G. (1977) *Chem. Biol. Interact.* **19,** 143–160
67. Smith, L. L. (1987) *Hum. Toxicol.* **6,** 31–36
68. Kuo, W. Y., and Tang, T. K. (1998) *Free Radic Biol. Med.* **24,** 1130–1138
69. Sittipunt, C. (2005) *Respir. Care* **50,** 383–385
70. Hoffer, E., Baum, Y., Tabak, A., and Taitelman, U. (1996) *Toxicol. Lett. (Shannon)* **84,** 7–12
71. van der Wal, N. A., van Oirschot, J. F., van Dijk, A., Verhoef, J., and van Asbeck, B. S. (1990) *Biochem. Pharmacol.* **39,** 1665–1671
72. Hagen, T. M., Brown, L. A., and Jones, D. P. (1986) *Biochem. Pharmacol.* **35,** 4537–4542
73. Tanaka, R. (2000) *J. Toxicol. Sci.* **25,** 199–204
74. McCarthy, S., Somayajulu, M., Sikorska, M., Borowy-Borowski, H., and Pandey, S. (2004) *Toxicol. Appl. Pharmacol.* **201,** 21–31
75. Johnson, D. K., Schillinger, K. J., Kwait, D. M., Hughes, C. V., McNamara, E. J., Ishmael, F., O'Donnell, R. W., Chang, M. M., Hogg, M. G., Dordick, J. S., Santhanam, L., Ziegler, L. M., and Holland, J. A. (2002) *Endothelium* **9,** 191–203
76. Higuchi, A., Yonemitsu, K., Koreeda, A., and Tsunenari, S. (2003) *Toxicology* **183,** 143–149
77. Shimada, H., Furuno, H., Hirai, K., Koyama, J., Ariyama, J., and Simamura, E. (2002) *Arch. Biochem. Biophys.* **402,** 149–157
78. Hirai, K., Ikeda, K., and Wang, G. Y. (1992) *Toxicology* **72,** 1–16
79. Mostert, V., Hill, K. E., and Burk, R. F. (2003) *FEBS Lett.* **541,** 85–88
80. Gromer, S., Urig, S., and Becker, K. (2004) *Med. Res. Rev.* **24,** 40–89
81. Xia, L., Nordman, T., Olsson, J. M., Damdimopoulos, A., Bjorkhem-Bergman, L., Nalvarte, I., Eriksson, L. C., Arner, E. S., Spyrou, G., and Bjornstedt, M. (2003) *J. Biol. Chem.* **278,** 2141–2146
82. Zhou, M., Diwu, Z., Panchuk-Voloshina, N., and Haugland, R. P. (1997) *Anal. Biochem.* **253,** 162–168